Published online 28 November 2017

Nucleic Acids Research, 2018, Vol. 46, No. 4 ***e24***
doi: 10.1093/nar/gkx1218

DNA terminal structure-mediated enzymatic reaction for ultra-sensitive discrimination of single nucleotide variations in circulating cell-free DNA

Tongbo Wu[1,†], Wei Chen[1,†], Ziyu Yang[1], Haocheng Tan[1], Jiayu Wang[1], Xianjin Xiao[2], Mengyuan Li[1] and Meiping Zhao[1,*]

[1]Beijing National Laboratory for Molecular Sciences and MOE Key Laboratory of Bioorganic Chemistry and Molecular Engineering, College of Chemistry and Molecular Engineering, Peking University, Beijing 100871, China and [2]Family Planning Research Institute/Center of Reproductive Medicine, Tongji Medical College, Huazhong University of Science and Technology, Wuhan 430030, China

Received July 29, 2017; Revised November 08, 2017; Editorial Decision November 17, 2017; Accepted November 23, 2017

ABSTRACT

Sensitive detection of the single nucleotide variants in cell-free DNA (cfDNA) may provide great opportunity for minimally invasive diagnosis and prognosis of cancer and other related diseases. Here, we demonstrate a facile new strategy for quantitative measurement of cfDNA mutations at low abundance in the cancer patients' plasma samples. The method takes advantage of a novel property of lambda exonuclease which effectively digests a 5′-fluorophore modified dsDNA with a 2-nt overhang structure and sensitively responds to the presence of mismatched base pairs in the duplex. It achieves a limit of detection as low as 0.02% (percentage of the mutant type) for *BRAF*V600E mutation, *NRAS*Q61R mutation and three types of *EGFR* mutations (G719S, T790M and L858R). The method enabled identification of *BRAF*V600E and *EGFR*L858R mutations in the plasma of different cancer patients within only 3.5 h. Moreover, the terminal structure-dependent reaction greatly simplifies the probe design and reduces the cost, and the assay only requires a regular real-time PCR machine. This new method may serve as a practical tool for quantitative measurement of low-abundance mutations in clinical samples for providing genetic mutation information with prognostic or therapeutic implications.

INTRODUCTION

Genomic alterations in cell-free DNA (cfDNA) in blood may provide real-time information on tumor progression, treatment effectiveness and cancer metastasis risk (1–3). Liquid biopsies that detect and quantify slight variations in DNA sequence have distinct advantages over tissue biopsy for their convenience, minimal invasiveness, and reproducibility (4–6). The mutations in cfDNA, commonly single nucleotide substitutions, are usually present at an abundance level close to or even lower than 1%, which is too low for the Sanger sequencing or pyrosequencing coupled with conventional PCR amplification. Much effort has been made to develop novel sequencing technologies or selective PCR methods to improve the assay sensitivity to minor mutant alleles among a large excess of normal wild-type (WT) alleles. Novel sequencing methods such as whole-genome sequencing (WGS), (7) tagged-amplicon deep sequencing (TAM-Seq) (8,9) and cancer personalized profiling by deep sequencing (CAPP-Seq) (10) achieved lower limits of detection (LOD) in the range from 0.02% to 2% (percentage of the mutant type as a fractional abundance) and enabled correlation of mutation types and levels with disease status. However, these methods are time-consuming (from days to weeks) and expensive. For selective PCR approaches, such as digital PCR (dPCR) (9), co-amplification at lower denaturation temperature-PCR (COLD-PCR), (11) amplification refractory mutation system PCR (ARMS-PCR), (12,13) beads, emulsion, amplification, magnetics (BEAMing) (14) and locked nucleic acid (LNA) assisted wild-type blocking PCR (LNA-PCR) (15,16), the LODs are generally from 0.01% to 3%, but complex design of the primer and precise control of temperature are often required. In comparison with the normal dPCR which has an LOD of 0.1%, (9) the droplet digital PCR (ddPCR) reached an LOD as low as 0.001–0.005% (17,18). However, dPCR assay depends on expensive instruments and time-consuming steps and ddPCR relies on additional devices for the droplet formation and detection. The LOD of SNPase-AMRS-qPCR (13) even reached 0.0005% by using the novel poly-

*To whom correspondence should be addressed. Tel: +86 10 62758153; Fax: +86 10 62751708; Email: mpzhao@pku.edu.cn
†These authors contributed equally to this work as first authors.

merase SNPase to suppress the background signal of normal AMRS-PCR. However, it required two rounds of PCR amplification and false negative signals occurred when detecting the mutations at low abundances.

Recently, a new electrochemical method based on the hybridization of circulating tumor DNA (ctDNA) with single-stranded DNA clutch probes or peptide nucleic acid (PNA) clamps has been developed and provides LODs between 0.01% and 0.1% (19–21). It allowed the detection of ctDNA without the need for PCR amplification. However, the assay was limited by multiple off-line sample pretreatment steps and large fluctuations in the current signals (21). Taking advantage of the sensitive response of different nucleases to the presence of mismatched base pairs in the DNA substrate, enzyme-assisted single nucleotide mutation detection methods have shown very competitive results in the identification of DNA mutations at very low abundances (0.01–0.1%) (22,23). However, for some target DNA mutations, the existing approaches rely on expensive fluorescent probes because the fluorophore needs to be labeled at the non-thymine bases within the probe sequence. By contrast, it would be much easier to attach the fluorophore to the phosphate backbone at the end of the probe. Moreover, the linearity between the fluorescence signals of existing probes and the mutation level in the low-abundance range (<1.0%) was not satisfactory, thus limiting their capability in providing reliable quantitative information of the low-level mutation in clinical samples.

In this work, we disclose a very interesting new property of lambda exonuclease (λ exo), which provides an inherently powerful discrimination capability toward the presence of a mismatched base in the target DNA sequence. Within a simple and mild enzymatic reaction solution, discrimination factors (the ratio of signal induced by perfect-match target to that induced by single-base mismatched target) as high as 220 to 1420 were obtained for different types of mismatched base pairs. By coupling with only a single round of regular PCR, the method allowed for rapid and quantitative measurement of the low-abundance mutations with an LOD down to 0.02%. It enabled identification of an *EGFR*L858R mutation (1.1 ± 0.1%) in the plasma of a lung cancer patient and a *BRAF*V600E mutation (0.9 ± 0.1%) in the plasma of a thyroid cancer patient, respectively, within only 3.5 h. This new method may serve as a practical tool for quantitative measurement of the low-abundance mutations in the cfDNA from plasma samples, and thus holds great potential for wide clinical applications.

MATERIALS AND METHODS

Materials

Lambda exonuclease (λ exo), Exonuclease I (Exo I), Vent DNA polymerase (Vent), Lambda Exonuclease Reaction Buffer (67 mM Glycine-KOH (pH 9.4 @ 25°C), 2.5 mM $MgCl_2$, 50 μg/ml BSA) and ThermoPol Reaction Buffer (20 mM Tris–HCl, 10 mM KCl, 10 mM $(NH_4)_2SO_4$, 2 mM $MgSO_4$ and 0.1% Triton X-100, pH 8.8 @ 25°C) were purchased from New England Biolabs (MA, USA). Taq DNA polymerase (Taq), Pfu DNA polymerase (Pfu) and dNTPs were purchased from Tiangen Biotech Co. (Beijing, China). DNA strands were synthesized and purified by HPLC (Sangon Biotech Co., China). The sequences of all the probes and targets that have been studied in this work are summarized in Supplementary Table S1. DNase/RNase free deionized water purchased from Tiangen Biotech Co. (Beijing, China) was used with all the experiment.

Digestion of dsDNA substrate with different 5′ ends and mismatched base pairs by λ exo (Figure 1B and Supplementary Figure S2)

To a 200 μl PCR tube, 39 μl of water, 5 μl of 10 × ThermolPol Reaction Buffer, 2 μl of probe (10 pmol) and 1 μl of target ssDNA (5 pmol) were added and mixed well. The solution was heated to 85°C and then gradually cooled down to 37°C. Then 3 μl of λ exo (1.67 U) was added and the detection was performed at 37°C on a Rotor-Gene Q 5plex HRM Instrument (QIAGEN, Hilden, Germany) with gain level of 8. Fluorescence intensity was measured once a cycle (5 s per cycle) for 240 cycles. The excitation and emission wavelengths were set to 470 and 510 nm, respectively. The rate of fluorescence increase was determined by the slope of the linear portion of the time curve.

Detection of different target sequences by 5′-overhang probe (Figures 1C, 3, 4, Supplementary Figure S3, S9A, Tables S2 and S3)

To a 200 μl PCR tube, 39 μl (for Figures 1C and 3B) or 37 μl (for Figures 3A, 4, Supplementary Figure S3, S9A, Tables S2 and S3) of water, 5 μl of 10 × Lambda Exonuclease Reaction Buffer, 2 μl of probe (10 pmol) and 1 μl of target ssDNA (5 pmol) were added and mixed well. For Figures 3A and 4, Supplementary Figure S9A and the mismatch types of C:C, T:T, T:G in Supplementary Table S2, additional 2 μl of $(NH_4)_2SO_4$ was added to the reaction buffer at a final concentration of 30 mM. For the mismatch types of C:T, C:A, T:C in Supplementary Table S2, additional 2 μl of $(NH_4)_2SO_4$ was added to the reaction buffer at a final concentration of 40 mM. After the same heating-annealing procedures as described above, 3 μl of λ exo (5 U) was added and the detection was performed at 37°C as described above with gain level of 8.

Detection of low abundance *BRAF*V600E, *NRAS*Q61R, *EGFR*T790M, *EGFR*G719S and *KRAS*G12X (X = R, S or C) point mutations (Figure 2A, Supplementary Figures S4, S5 and S9B)

To a 200 μl PCR tube, 37 μl of water, 5 μl of 10 × Lambda Exonuclease Reaction Buffer, 2 μl of probe (10 pmol), 1 μl of mixed target ssDNA with different MT abundances (total amount 5 pmol), 2 μl of $(NH_4)_2SO_4$ (at a final concentration of 10 mM for Figure 2A and Supplementary Figure S5, 20 mM for Supplementary Figure S4 and 30 mM for Supplementary Figure S9B) was added and mixed well. For Supplementary Figure S5C and D, additional blocker (20 pmol) was added. After the heating-annealing procedure same as above, 3 μl of λ exo (5 U) was added and the detection was performed at 37°C in the same manner as described above (gain = 10).

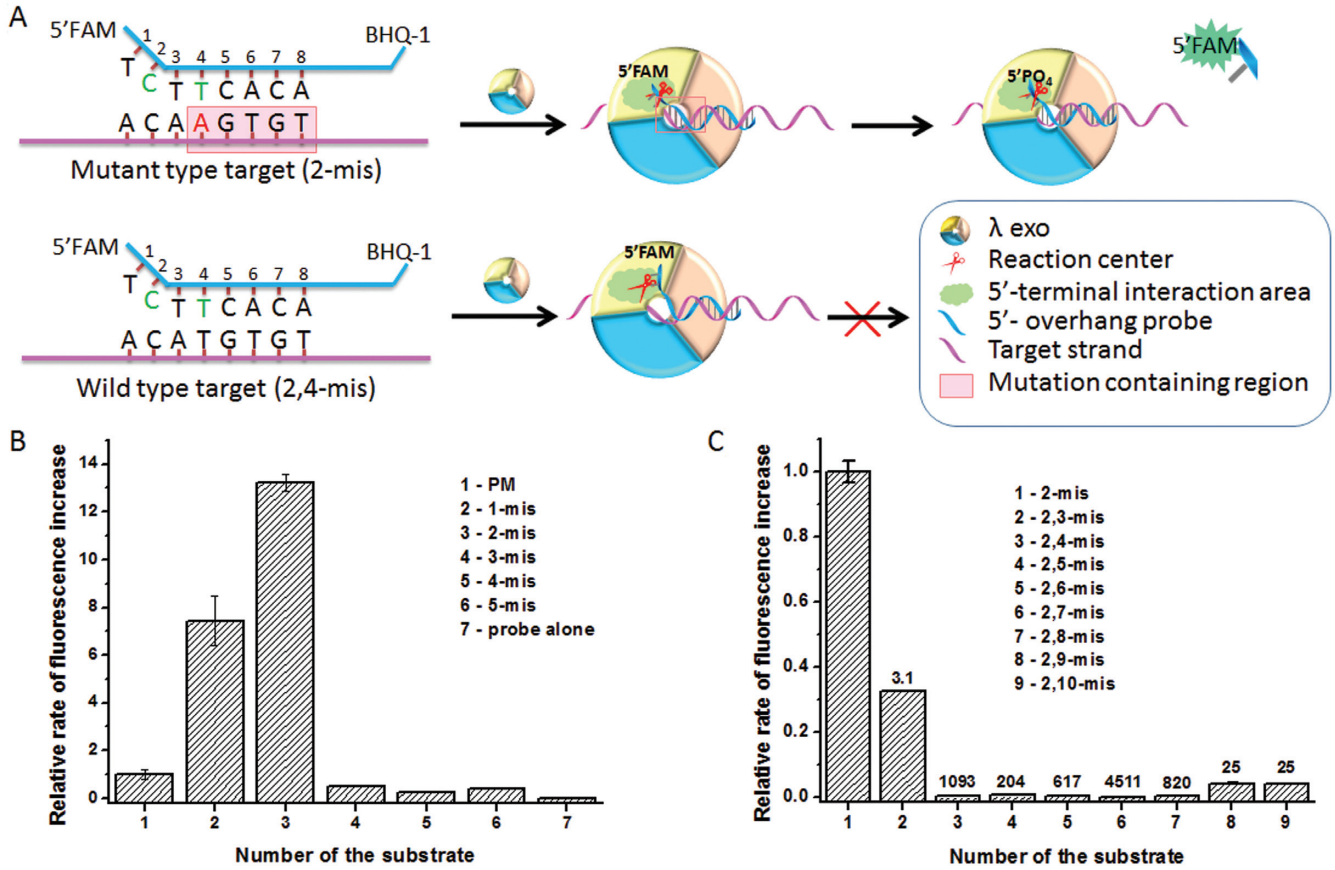

Figure 1. (**A**) Schematic depiction of the interactions between λ exo and the DNA substrates with different 5′ terminal structures. (**B**) Relative digestion rates of different 5′-FAM substrates with different mismatches by λ exo. The rate of fluorescence increase of PM substrate was set as 1. Error bars represent the standard deviation from experiments performed in triplicate. PM: perfectly matched dsDNA. (**C**) Reaction rates between λ exo and the 5′-FAM 2-mis dsDNA substrate with an additional mismatched base in the duplex. The rate of fluorescence increase of the 2-mis substrate was set as 1. The probe used was P1-5′-FAM and the complementary strands were C1 series (Supplementary Table S1).

Detection of low abundance *BRAF*V600E mutation in circulating cell free DNA (cfDNA) in the plasma of cancer patients (Figure 2B & C, Supplementary Figures S6 and S7)

The cfDNA was extracted from 100 μl of plasma using the DNeasy Blood & Tissue Kit (QIAGEN, Hilden, Germany) and quantified with NanoDrop 2000 UV-Vis Spectrophotometer (Thermo Fisher Scientific Inc., MA, USA). To a 200 μl PCR tube, 26.5 μl of water, 5 μl of 10× ThermolPol Reaction Buffer, 4 μl of dNTPs (10 nmol), 1 μl of forward primers (20 pmol), 1 μl of reverse primers (20 pmol), 1 μl of the dsDNA from the plasma sample (0.05 amol) or the mixed standard sample of synthesized target ssDNA (total amount 0.05 amol) with different MT abundances, 0.5 μl of Vent (1.25 U) were added and mixed well. PCR procedure (94°C 30 s, 60°C 30 s, 72°C 20 s, 25 cycles) was performed on a Rotor-Gene Q 5plex HRM Instrument. After the PCR amplification, 1 μl of Exo I (5 U) was added to remove the unreacted primers, followed by inactivation at 85°C for 10 min. Then 3 μl of λ exo (5 U) was added to digest the strand containing 5′-PO_4 in the duplex products for 20 min at 37°C. The obtained ssDNA in the solution was then extracted by TIANquick Mini Purification Kit (Tiangen Biotech Co., Beijing, China) and quantified with NanoDrop 2000 UV-Vis Spectrophotometer. Then the mutation detection was performed in the same manner as described above.

Detection of *EGFR*L858R mutation in genomic DNA from the tissue and cfDNA in the plasma of a lung cancer patient (Figure 2D–F and Supplementary Figure S8)

The genomic DNA was extracted from the tumor tissue of a lung cancer patient by using TIANamp Micro DNA Kit purchased from Tiangen Biotech Co. The cfDNA was extracted from 100 μl of plasma from the same patient using the DNeasy Blood & Tissue Kit. Then the extracted DNA was quantified with NanoDrop 2000 UV-Vis Spectrophotometer. PCR and post-PCR treatment procedures were conducted the same as *BRAF*V600E detection described above for the extracted DNA and the synthesized standards with different mutation abundance, except that the PCR cycles were 94°C 16 s, 56.5°C 16 s, 72°C 25 s, 50 cycles. The *EGFR*L858R mutation was performed after the target ssDNA obtained from the post-PCR treatment was quantified. To a 200 μl PCR tube, 32 μl of water, 5 μl of 10 × Lambda Exonuclease Reaction Buffer, 2 μl of probe (10 pmol), 5 μl of target ssDNA (5 pmol), 2

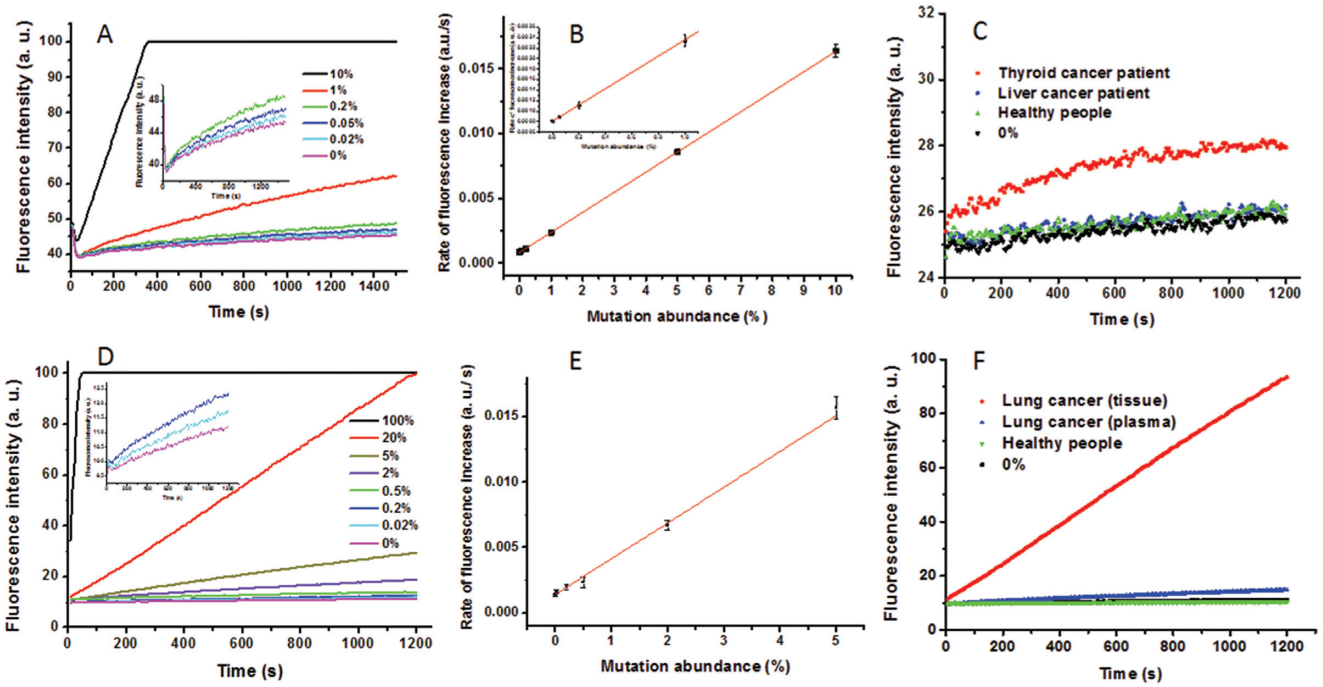

Figure 2. (**A**) Fluorescence intensity responses of P6-*BRAF*V600E in the detection of *BRAF*V600E(1799T>A) mutation at different abundances (from 0% to 10%). The insert zoomed in the curves of 0.2%, 0.05%, 0.02% and 0%. 100% means the tested strands are all mutant type (T2-*BRAF*V600E-MT-A). 0% means the tested strands are all wild type (T2-*BRAF*V600E-WT-T). (**B**) Calibration curve of the rate of fluorescence increase of P6-*BRAF*V600E versus different levels of *BRAF*V600E mutation (T2-*BRAF*V600E-PCR-MT). The zoom-in insert shows the data points at low mutation levels (0%, 0.05%, 0.2% and 1.0%). (**C**) Fluorescence intensity responses of the P6-*BRAF*V600E in detection of *BRAF*V600E(1799T>A) mutation in the cfDNA obtained from different samples. (**D**) Fluorescence intensity response of P10-*EGFR*L858R in the detection of *EGFR*L858R (2573T>G) mutation at different abundances (from 0% to 100%). The insert zoomed in the curves of 0.2%, 0.02% and 0%. 100% means the tested strands are all mutant type (T6-*EGFR*L858R-PCR-MT-G). 0% means the tested strands are all wild type (T6-*EGFR*L858R-PCR-WT-T). (**E**) Calibration curve of the rate of fluorescence increase of P10-*EGFR*L858R versus different levels of *BRAF*V600E mutation (T6-*EGFR*L858R-PCR-MT-G). (**F**) Fluorescence intensity responses of the P10-*EGFR*L858R in detection of *EGFR*L858R(2573T>G) mutation in different samples. The sequences of the probe and targets were listed in Supplementary Table S1. Error bars represent the standard deviation from experiments performed in triplicate.

μl of blocker (20 pmol),1 μl of $(NH_4)_2SO_4$ (at a final concentration of 10 mM) was added and mixed well. After the heating-annealing procedure same as above, 3 μl of λ exo (10 U) was added and the detection was performed at 37°C in the same manner as described above (gain = 10).

RESULTS AND DISCUSSION

Terminal structure of the 5′ end of dsDNA substrate substantially affects the digestion rate by λ exo

λ exo (Figure 1A, toroid) is a 5′ to 3′ exonuclease trimer which forms a toroid structure and digests one strand of the double-stranded DNA (dsDNA) with a 5′-PO_4 end (24,25). It has been widely accepted that the 5′-PO_4 end is essential for λ exo to processively digest the single-strand substrate via the electrostatic interactions with the positively charged pocket in λ exo (Figure 1A, light green area in the toroid) (26,27). In our work, however, we found that when we substituted the 5′-PO_4 end with a 5′-FAM end (Supplementary Figure S1A), and incorporated a mismatched base at the second position from the FAM-labeled 5′ end, the 5′-FAM 2-mis strand (shown in blue ribbon, Figure 1A) in a DNA duplex could also be quickly digested by λ exo. The reaction rate was about 14 times faster than that of the perfectly matched 5′-FAM dsDNA substrate (Figure 1B). By contrast, the digestion rates of other single-mismatched dsDNA with the altered base located at the third to fifth positions from the FAM-labeled 5′ end (3-mis, 4-mis or 5-mis) by λ exo were all remarkably lower than that of the 2-mis duplex (Figure 1B). The digestion rate of the 5′-FAM ssDNA probe alone was only 1.1% of that of the PM duplex, thus the background signal of the probe was almost negligible in comparison with the signal from the 2-mis duplex.

According to the previous work, (28) dsDNA with a penultimate mismatch may be regarded as bearing a two-nucleotide (2-nt) overhang structure. To confirm such a property, we tested several other dsDNA substrates which also had a 2-nt overhang structure. As shown in Supplementary Figure S2A, all the tested 5′-FAM substrates with a 2-nt overhang structure could be efficiently digested by λ exo, indicating that the special terminal structure at 5′ end of the dsDNA could also initiate the digestion reaction and lead to cleavage of the 5′-FAM. The reaction rates were even at the same level as that of the 5′-PO_4 PM substrate, which was traditionally believed as the most suitable substrate for λ exo. Similar results were also obtained for other probes with 5′-FAM end (Supplementary Figure S2B) or 5′-BHQ-1 end (Supplementary Figure S2C). These results substantially confirmed that the 5′ terminal 2-nt overhang together with a chemical tag could replace the role of 5′-PO_4 and

pull the 5′ end substrate strand to the reaction center (Supplementary Figure S1B).

Sensitive discrimination of the single nucleotide mutation by using the 5′-overhang probe and λ exo

We further investigated the reactions between λ exo and the 5′-FAM 2-mis substrate with the addition of a second mismatched base near the 2-mis site in the 5′-FAM strand. Interestingly, the digestion rates of 2,*x*-mis ($x = 4$–8) substrates all dramatically decreased compared to that of the 2-mis substrate (Figure 1C). The ratio of the signal of the 5′-FAM 2-mis substrate to that of the 2,*x*-mis substrate were observed to be all higher than 200 and some even reached as high as 4511. Such difference was remarkably larger than those obtained for the 5′-PO_4 dsDNA substrate which contained one or two mismatched bases (29), indicating that for the 5′-FAM 2-nt-overhang terminal structure, the enzyme required a more precisely hybridized duplex to effectively digest the substrate. Thus the reaction system was much more sensitive to the presence of additional mismatched base pair within the duplex. Based on this unique capability, we propose a flexible 5′-FAM overhang probe to distinguish the known or new single nucleotide variation at known or unknown positions of a target sequence.

First, we focused on detection of single nucleotide mutation of known types at fixed positions based on the large difference between 5′-FAM 2-mis substrate and 5′-FAM 2,*x*-mis ($x = 4$–8) substrate. For this purpose, we set the 2-mis target as the mutant type (MT) sequence and 2,*x*-mis ($x = 4$–8) target as the wild type (WT) sequence. As illustrated in Figure 1A, the 5′-FAM probe has a mismatched base at Position 2 (shown in green) with both of the MT and WT targets. The base at one of the positions from 4 to 8 in the 5′-FAM probe was designed to be matched with the altered base in the MT sequence while mismatched with the native one in the WT sequence (In Figure 1A, the base at Position 4 was marked as an example). Thus, the resultant probe/MT hybrid would have a 5′-FAM 2-nt overhang structure and be digested very fast; while the probe and the WT would form a 2,*x*-mis unstable hybrid structure, which were digested notably slower. Using P1-5′-FAM and P5-5′-FAM-4T as a model 5′-overhang probe and the base at position 4 from the 5′ end of the probe to match with the target base in the MT sequence, we altered the base type in the WT sequence (Supplementary Table S1, T1 series) and measured the discrimination factors (DF, defined as the ratio between the signal of the MT sequence and that of the WT sequence) between the 5′-FAM 2-mis probe/MT hybrid and 5′-FAM 2,4-mis probe/WT hybrid. Under the optimized reaction buffer conditions (as described in the Supporting Information), the DFs for all the six different mismatch types were observed to be between 200 and 1420 (Supplementary Table S2).

Following the above line of thought, we synthesized two new 5′-overhang probes (P6-*BRAF*V600E and P7-*NRAS*Q61R) to detect two genetic mutations associated with diseases. *BRAF*V600E (NM_004333.4:c.1799T>A) is related to papillary thyroid carcinoma, non-small cell lung cancer (NSCLC), carcinoma of colon, astrocytoma and malignant melanoma (30–34). *NRAS*Q61R (NM_002524.4:c.182A>G) is related to neurocutaneous melanosis, epidermal nevus syndrome, thyroid cancer and NSCLC (31,35–38). The DFs were observed to be as high as 611 for *BRAF*V600E and 2153 for *NRAS*Q61R, which enabled detection of *BRAF*V6000E (Figure 2A and B) and *NRAS*Q61R (Supplementary Figure S4) mutations at abundances as low as 0.02% (percentage of the MT).

Then we further extended the method to detect *EGFR*-associated mutations. *EGFR* mutations are related to many cancers such as NSCLC (39), colon cancer (40) and breast cancer (41). The single nucleotide mutations such as *EGFR*L858R, *EGFR*T790M and *EGFR*G719S are widely used for NSCLC diagnosis and treatment evaluation (42,43). As these mutation sites are buried within GC-rich sequence, it is difficult to distinguish them by conventional methods. We designed three 5′-overhang probes (P8-*EGFR*T790M, P9-*EGFR*G719S and P10-*EGFR*L858R) to detect these mutations. The *EGFR*T790M mutation (NM_005228.4:c.2369C>T) was relatively easy to discriminate, the DF was 226 and the limit of detection (LOD) was 0.02% (Supplementary Figure S5A & B). For *EGFR*G719S (NM_005228.4:c.2155G>A), the mismatched base pair formed at Position 4 in the probe/WT hybrid was a stable T:G mismatch, which was relatively hard to be discriminated. So we introduced a blocker which had the same length as the probe and perfectly matched with the WT sequence to suppress the background signals (44). As the probe had two mismatches with WT, the blocker would significantly impede the hybridization of probe and WT. The resultant DF was 286 and the LOD reached 0.02% (Supplementary Figure S5C and D).

For *EGFR*L858R (NM_005228.4:c.2573T>G), the mutation site is surrounded by four consecutive G/C base pairs at each side, thus the discrimination of this mutation is most difficult. In our experiment, we found that if the first base at the 5′ end (Position 1) of the 5′-overhang probe was G or C, the reaction rate of the 2-mis probe/MT hybrid would be very slow, most likely because the G:C base pair was too stable to form the 2-nt overhang structure at the 5′ end. So we employed probe P10-*EGFR*L858R to avoid the formation of G:C or C:G basepair at Position 1. The probe formed 2-mis hybrid with MT and a 2,6-mis hybrid with WT. With the addition of blocker to suppress the background signals of WT, very high DF (996) was obtained and the LOD was 0.02% (Figure 2D and E)

Above results substantially demonstrated that the 5′-FAM overhang probe can be used to detect single nucleotide mutation of known types at fixed positions and provide very high DFs and low LODs. Since the sequence of the probe can be flexibly changed according to the position of mutation site and the surrounding sequences, the 5′-overhang probe holds the potential to detect mutations located at any position of the target sequence.

Quantification of the muation level of *BRAF*V600E and *EGFR*L858R in cfDNA in the plasma of cancer patients

Encouraged by above results, we further applied the method to measure the abundance of *BRAF*V600E mutation in the cfDNA from the plasma of thyroid cancer patients. We extracted the cfDNA from the plasma samples of thyroid

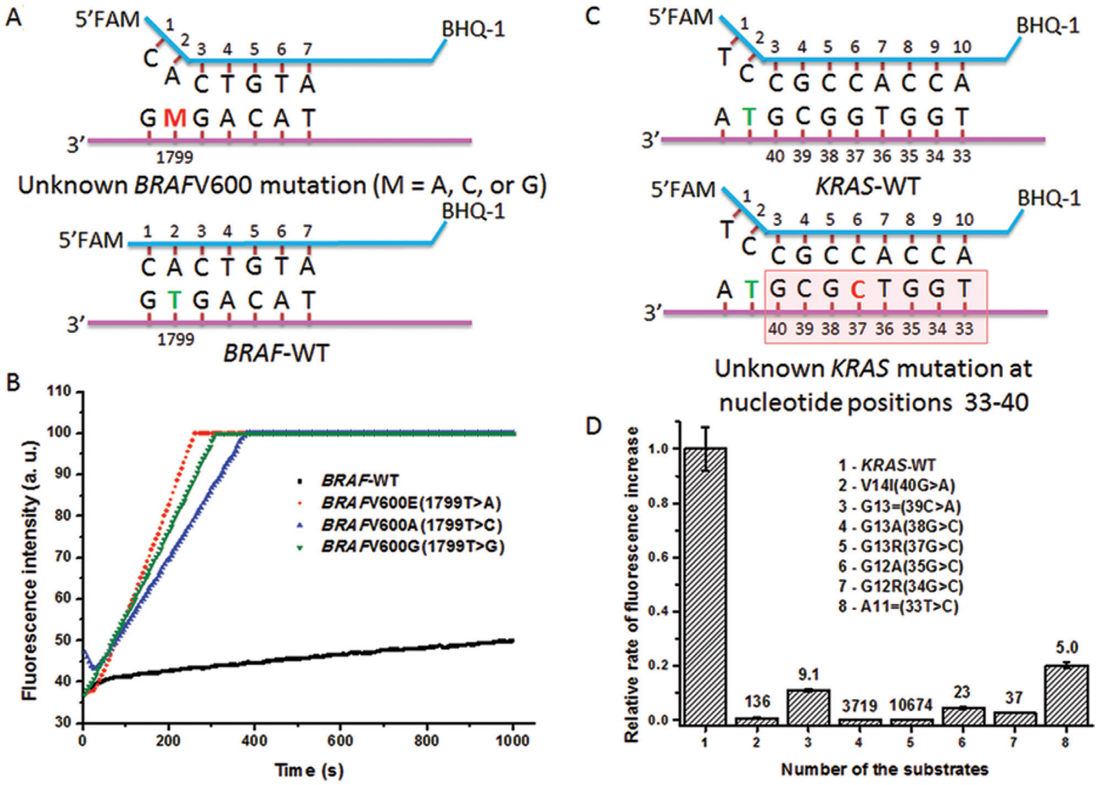

Figure 3. (**A**) Schematic depiction of the structures of the probe/*BRAF*-MT and probe/*BRAF*-WT. WT: wild-type target sequence. MT: mutant-type target sequence. (**B**) Fluorescence intensity responses of the P8-*BRAF*V600-unknown to the *BRAF*-WT and three *BRAF*V600(1779T) mutations. (**C**) Schematic depiction of the structures of the probe/*KRAS*-WT and probe/*KRAS*-MT. The mutation may occur in the region from position 33 to 40 shown in light red. (**D**) Detection of seven possible mutations in the codon 11 to codon 14 area in *KRAS*. The DFs (WT to MT signal ratio) were indicated above the columns. Error bars represent the standard deviation from experiments performed in triplicate. The probe used was P13-*KRAS*-multiple unknown and the targets were T9 series. The sequences of the probes and targets were listed in Supplementary Table S1.

cancer patients, liver cancer patients and healthy individuals, respectively. After a single round of conventional PCR and enzymatic treatment, the amplified *BRAF*V600E related sequences were obtained and used for the subsequent mutation detection (see details in the MATERIALS AND METHODS section). It was observed that the polymerase employed for the PCR procedure had significant influences on the PCR products. By comparison of three different DNA polymerases (Taq, Pfu and Vent), we found that the fidelity of Vent was much higher than those of other two tested polymerases. From the experimental results shown in Supplementary Figure S6, the background of 100% WT after PCR procedure with Vent polymerase was very low, which was almost similar to that of the no-target control. So we chose Vent to perform the PCR amplification before the mutation detection. We also tested another high fidelity polymerase (Q5 polymerase), the results were generally similar to those of the Vent DNA polymerase, indicating that the influences of mutations possibly introduced during the PCR amplification on the results of our target sequence were negligible. For the detection of very low-abundance mutations, high fidelity polymerases should be employed to conduct the PCR procedure.

From Figure 2C, the increased rate of fluorescence signals of *BRAF*V600E mutation in the cfDNA from plasma of the thyroid cancer patient was much faster than those from the liver cancer patient and the healthy people. We performed *t* test ($n = 3$) for the two cancer samples (Supplementary Figure S7). The *BRAF*V600E mutation level detected in the thyroid cancer patient sample was found to be significantly different from that in the healthy people sample ($t = 44$, $P < 0.001$); while the *BRAF*V600E mutation level detected in the samples from the liver cancer patient and the healthy people were generally similar ($t = 0.408$). Then we prepared the calibration curve by using the synthesized target MT and WT sequences to obtain standard samples with different mutation abundances and performing the PCR and post-PCR treatment in the same way as above. The rates of fluorescence increase of these standards showed excellent linear relationship with the mutation abundance in the range from 0.05% to 10% ($R^2 = 0.9999$, Figure 2B), thus the abundance of *BRAF*V600E mutation in the cfDNA from plasma of the thyroid cancer patient was quantitatively measured to be $0.9 \pm 0.1\%$. The whole procedure (from extraction of the cfDNA from the plasma samples to giving out the quantitative results of the mutation level) took <3.5 h, which was much shorter than the sequencing methods, selective PCR-based approaches and ddPCR technology.

To demonstrate the applicability of the method to different target sequences and types of cancer, we further employed P10-*EGFR*L858R to measure the abundance of the *EGFR*L858R mutation in the cfDNA extracted from

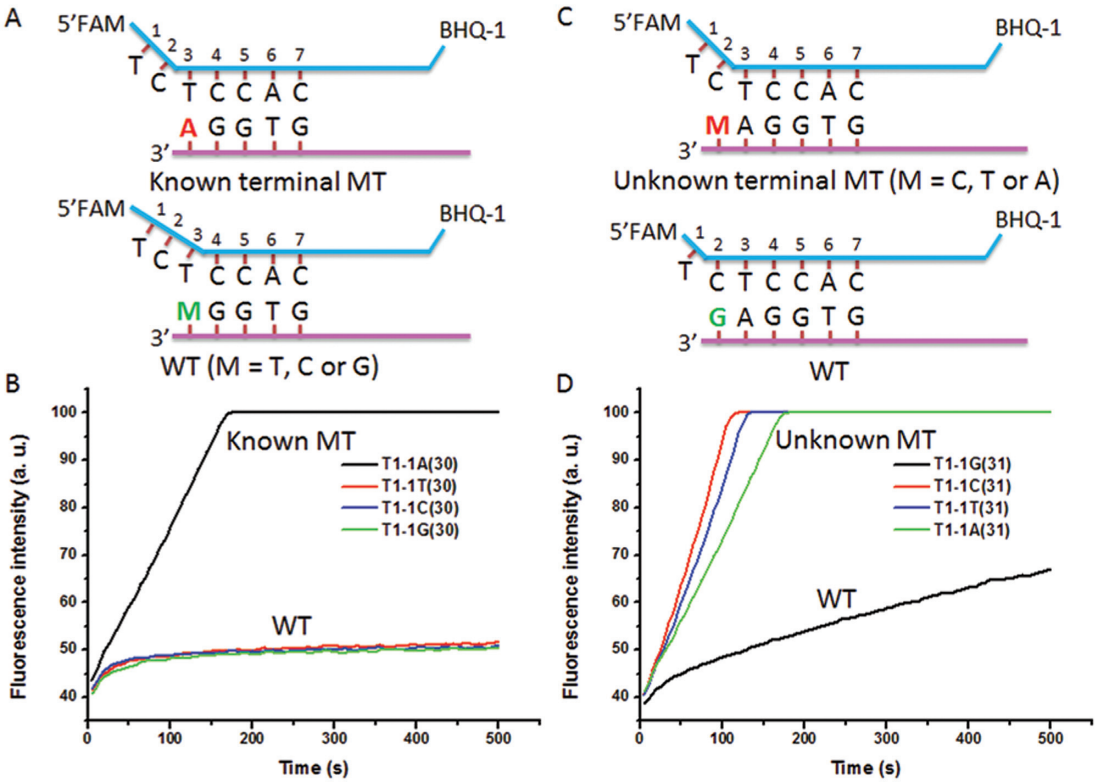

Figure 4. (**A**) Schematic depiction of the structure of the 5′-overhang probe used for the detection of known mutations at the 3′ end of the target sequence. WT: wild-type target sequence. MT: mutant-type target sequence. (**B**) Fluorescence intensity responses of the P1–5′-FAM to the WT and MT with known-type terminal mutation (T1–1A (30)). (**C**) Schematic depiction of the structure of the 5′-overhang probe used for the detection of unknown mutations at the 3′ end of the target sequence. (**D**) Fluorescence intensity responses of the P1–5′-FAM to the WT and MT with terminal mutation of unknown types (T1–1C (31), T1–1C (31) or T1–1T (31)). The sequences of the probe and targets were listed in Supplementary Table S1.

the plasma of a lung cancer patient. For comparison, genomic DNA extracted from the tumor tissue from the same patient was also measured. As shown in Figure 2F, the *EGFR*L858R mutation level detected in the plasma and tissue samples from the lung cancer patients were both significantly higher than that from the healthy people and control sample (0% MT). Based on the standard curve shown in Figure 2E ($R^2 = 0.99$), the abundance of *EGFR*L858R mutation in the cfDNA from the plasma was 1.1 ± 0.2%. The genomic DNA mutation level in the tumor tissue from the same patient was measured to be as high as 26 ± 2%, which was consistent with that obtained by using Sanger sequencing (∼25%, Supplementary Figure S8). These results substantially prove that our method can be used for quantitative liquid biopsy and provide the same important information as the tissue biopsy for disease diagnosis and treatment.

Detection of mutation of unknown types or at unknown positions

Next, we attempted to use the 5′-overhang probe to detect the single nucleotide mutation of unknown types or at unknown positions, which was also frequently needed in the clinical diagnosis. For this purpose, we first figured out a new strategy to detect all the three possible unknown mutation types at a fixed position. As shown in Figure 3A, the probe was designed to be perfectly matched with the WT. Without the 2-nt overhang structure, the probe/WT was digested very slowly. For the mutant type, all the three possible MTs formed a mismatched basepair with the probe at Position 2. Due to the generation of a 2-nt overhang structure at the 5′-FAM end, the probe/MT were digested remarkably faster. The base T at position 1799 in *BRAF*V600 may mutate to A, C or G and form three different mutations, namely *BRAF*V600E, *BRAF*V600A and *BRAF*V600G. From the results shown in Figure 3B, one 5′-overhang probe could identify all the three unknown mutations with the DFs of 29, 18 and 22 respectively. The limits of detection reached 0.5% (Supplementary Figure S9A). This is far more sensitive than the commonly used sequencing methods for unknown mutation detection and comparable to the selective PCR method such as COLD-PCR. As shown in Supplementary Figure S9B, this unknown mutation detection strategy could also be applied to detect the three unknown mutations in *KRAS*G12 at position 34 and the DF achieved 40, 28 and 17 for *KRAS*G12R(34G>C), *KRAS*G12S(34G>A) and *KRAS*G12C(34G>T), respectively.

What's more challenging is to detect the unknown mutations at unknown positions. We further extended our strategy to detect the unknown mutations at up to eight possible positions by using the 5′-overhang probe within one experiment. According to previous study, multiple mutations may

occur in the codon 11 to codon 14 area in *KRAS*. As shown in Figure 3C, the probe is designed to have a mismatch with the WT sequence at Position 2, so the probe/WT duplex with the 2-nt overhang structure could be quickly digested by λ exo. With additional mismatched bases present in the region between Position 3 to 10 of the probe, the digestion rates of resultant probe/MT significantly decreased (Figure 3D). For the codon 11 to codon 14 area in *KRAS*, the unknown mutations at the seven possible nucleotide positions (between 33 and 40) could all be clearly identified with the DFs ranged from 5.0 to 10674. In comparison with other methods for the detection of unknown mutation at unknown positions, above strategy is much easier and time-saving, thus holds great potential for rapid preliminary screening of the mutations.

Detection of mutation located on the 3′ terminus of the target sequence

Another difficult issue in DNA mutation detection is to discriminate the mutations located at the end of a target sequence, as the terminal mismatch only slightly affects the melting temperature of the dsDNA. The decrease of free energy caused by various terminal mismatches was found to be <1 kcal/mol, which was actually within the variation of free-energy changes for the base pairing between two DNA strands with different sequences (45,46). Thus, the reported DFs for terminal mismatch were all lower than 10 (47–50). The terminal structure-dependent response property of the 5′-overhang probe makes it possible to identify known and unknown mutations at the 3′ terminus of the targets. As shown in Figure 4A, for known mutations, the 5′-overhang probe was designed to form a 5′-FAM 2-nt protruding end in the probe/MT duplex. The base T at the third position from the 5′ end (Position 3) of the probe was designed to be matched with the known 3′-terminal base (A) of the MT sequence, thus it would form a mismatch with the base (T, C or G) at 3′-end of the WT sequence. From Figure 4B, the probe/MT duplex bearing a 5′ 2-nt overhang structure was digested significantly faster than the probe/WT duplexes which formed a 3-nt overhang structure at the 5′-FAM end. The DFs were observed to be 66 for T:T, 146 for T:C and 120 for T:G mismatches, respectively. For unknown mutations at the 3′ end, as shown in Figure 4C, the 5′-overhang probe was designed to form a 5′-FAM 1-nt protruding end in the probe/MT duplex. The base C at Position 2 of the probe was designed to be matched with the known terminal base G at the 3′ end of the WT sequence, thus it was mismatched with the unknown base (C, T or A) at 3′ end of the MT sequence. Figure 4D shows that the probe/MT duplex bearing a 5′-FAM 2-nt overhang structure was digested much faster than the probe/WT duplexes which had a 1-nt overhang structure at the 5′-FAM end. The DFs were measured to be 131 for C:C, 106 for C:T and 75 for C:A, respectively. These results proved that for both known and unknown mutations at the 3′ terminus of the target sequence, the 5′-overhang probe showed much higher discrimination capability than the existing methods (47–50).

Taking the above results together, the 5′-overhang probe can be flexibly designed to detect known or unknown mutations at fixed positions or within a short region of the target sequence. They can also be used to detect mutations at the 3′ end of a target sequence with high DFs. In comparison with those previously reported fluorescent probes designed for post-PCR mutation detection (44,51–54), a distinct advantage of the 5′-overhang probe was the ultra-high sensitivity to low-abundance mutations, which should be attributed to the special interactions between λ exo and dsDNA with a 5′-FAM 2-nt overhang terminal structure. This unique structure brought the enzyme an extraordinary discrimination capability toward the presence of mismatched base pairs in the duplex region near the 5′ end, thus the DFs between MT and WT are very high.

Actually, the structure-specific recognition property has been previously reported for several other enzymes (55), such as the 5′ nuclease component of Taq DNA polymerase (56–58) and flap endonuclease 1 (FEN1) which can cleave the 5′ flap strand in the invasive displacement DNA complexes (59,60). By using the sensitive discrimination ability of FEN1 to the substrate structure change (61), a highly commercialized method, Invader Assay, has been developed (62), which is now widely used for single nucleotide polymorphisms (SNP) genotyping. (63,64) Compared with the invasive cleavage work, our method does not need an invasive strand to displace the 5′-overhang, and it achieves comparable performance to that of FEN1. The 5′-overhang probe we used also looks like the Taqman probe, as both of them have a fluorophore at the 5′ end and a quencher at the 3′ end. However, Taqman probe mainly differentiates the MT from WT based on the hybridization stability rather than the terminal structure-mediated enzymatic recognition property, thus the DFs are not as high as those of the 5′-overhang probe.

Another prominent feature of the new method was the simplicity and low cost. As it was much easier to attach the fluorophore to the phosphate backbone at the 5′ end than to label the internal especially non-thymine bases within the probe sequence, the cost savings were estimated to be 40–80%.

We also tested the 5′-BHQ-1 2-nt overhang dsDNA substrates with the FAM labeled at the 3′ end, which were also found to be digested faster than the 5′-BHQ-1 PM substrate without the overhang structure, though the digestion rates of 5′-BHQ-1 2-nt overhang duplexes were only about half of that of the 5′-PO_4 PM substrate. Under the reaction conditions, FAM was negatively charged while BHQ-1 was positively charged, suggesting that both the 2-nt overhang structure and the chemical property of the specific tag at the 5′ end of the dsDNA substrate have significant influences on the enzymatic reactions. The mechanisms for these interactions are under detailed investigation and will be reported elsewhere.

CONCLUSION

In conclusion, we have proposed a versatile terminal structure-mediated enzymatic reaction for ultra-sensitive discrimination of single nucleotide mutation. With the combination of a 2-nt overhang structure and a fluorophore labeled at the 5′ end, a 5′-overhang probe was flexibly designed and utilized to detect various mutations at a fixed position or within a short region of the target sequence. The

special 5′-terminal structure of the dsDNA enables λ exo to be more sensitive to the presence of mismatched base pairs in the duplex, thus the method offers excellent linear working range even in the low abundance range (<1.0%, percentage of the mutant type) and achieves a limit of detection as low as 0.02% for *BRAF*V600E mutation, *NRAS*Q61R mutation and three types of *EGFR* mutations (G719S, T790M, and L858R). It enabled identification of a *BRAF*V600E mutation (0.9 ± 0.1%) in the plasma of a thyroid cancer patient and an *EGFR*L858R mutation (1.1 ± 0.1%) in the plasma of a lung cancer patient, respectively, within only 3.5 h. The *EGFR*L858R mutation level in the tumor tissue from the same patient measured by our method (26 ± 2%) was in good agreement with that measured by Sanger sequencing (∼25%). Moreover, the terminal structure-dependent reaction greatly simplifies the probe design and reduces the cost, and the assay only requires a regular real-time PCR machine. The new method holds great potential in providing affordable and minimally invasive liquid biopsy for serial monitoring of genetic mutations that have prognostic or therapeutic implications.

SUPPLEMENTARY DATA

Supplementary Data are available at NAR Online.

FUNDING

National Natural Science Foundation of China [81571130100, 21575008, 21375004]; Beijing Municipal Natural Science Foundation [2152014] and the interdisciplinary medicine Seed Fund of Peking University. Funding for open access charge: National Natural Science Foundation of China.
Conflict of interest statement. None declared.

REFERENCES

1. Schwarzenbach,H., Hoon,D.S.B. and Pantel,K. (2011) Cell-free nucleic acids as biomarkers in cancer patients. *Nat. Rev. Cancer*, **11**, 426–437.
2. Murtaza,M., Dawson,S.J., Tsui,D.W.Y., Gale,D., Forshew,T., Piskorz,A.M., Parkinson,C., Chin,S.F., Kingsbury,Z., Wong,A.S.C. *et al.* (2013) Non-invasive analysis of acquired resistance to cancer therapy by sequencing of plasma DNA. *Nature*, **497**, 108–112.
3. Thierry,A.R., Mouliere,F., El Messaoudi,S., Mollevi,C., Lopez-Crapez,E., Rolet,F., Gillet,B., Gongora,C., Dechelotte,P., Robert,B. *et al.* (2014) Clinical validation of the detection of KRAS and BRAF mutations from circulating tumor DNA. *Nat. Med.*, **20**, 430–435.
4. Diaz,L.A. and Bardelli,A. (2014) Liquid biopsies: genotyping circulating tumor DNA. *J. Clin. Oncol.*, **32**, 579–586.
5. Wan,J.C.M., Massie,C., Garcia-Corbacho,J., Mouliere,F., Brenton,J.D., Caldas,C., Pacey,S., Baird,R. and Rosenfeld,N. (2017) Liquid biopsies come of age: towards implementation of circulating tumour DNA. *Nat. Rev. Cancer*, **17**, 223–238.
6. Siravegna,G., Marsoni,S., Siena,S. and Bardelli,A. (2017) Integrating liquid biopsies into the management of cancer. *Nat. Rev. Clin. Oncol.*, **14**, 531–548.
7. Leary,R.J., Sausen,M., Kinde,I., Papadopoulos,N., Carpten,J.D., Craig,D., O'Shaughnessy,J., Kinzler,K.W., Parmigiani,G., Vogelstein,B. *et al.* (2012) Detection of chromosomal alterations in the circulation of cancer patients with whole-genome sequencing. *Sci. Transl. Med.*, **4**, 162ra154.
8. Forshew,T., Murtaza,M., Parkinson,C., Gale,D., Tsui,D.W.Y., Kaper,F., Dawson,S.J., Piskorz,A.M., Jimenez-Linan,M., Bentley,D. *et al.* (2012) Noninvasive identification and monitoring of cancer mutations by targeted deep sequencing of plasma DNA. *Sci. Transl. Med.*, **4**, 136ra68.
9. Dawson,S.J., Tsui,D.W.Y., Murtaza,M., Biggs,H., Rueda,O.M., Chin,S.F., Dunning,M.J., Gale,D., Forshew,T., Mahler-Araujo,B. *et al.* (2013) Analysis of circulating tumor DNA to monitor metastatic breast cancer. *N. Engl. J. Med.*, **368**, 1199–1209.
10. Newman,A.M., Bratman,S.V., To,J., Wynne,J.F., Eclov,N.C.W., Modlin,L.A., Liu,C.L., Neal,J.W., Wakelee,H.A., Merritt,R.E. *et al.* (2014) An ultrasensitive method for quantitating circulating tumor DNA with broad patient coverage. *Nat. Med.*, **20**, 552–558.
11. Pinzani,P., Santucci,C., Mancini,I., Simi,L., Salvianti,F., Pratesi,N., Massi,D., De Giorgi,V., Pazzagli,M. and Orlando,C. (2011) BRAF(V600E) detection in melanoma is highly improved by COLD-PCR. *Clin. Chim. Acta*, **412**, 901–905.
12. Yancovitz,M., Yoon,J., Mikhail,M., Gai,W.M., Shapiro,R.L., Berman,R.S., Pavlick,A.C., Chapman,P.B., Osman,I. and Polsky,D. (2007) Detection of mutant BRAF alleles in the plasma of patients with metastatic melanoma. *J. Mol. Diagn.*, **9**, 178–183.
13. Stadler,J., Eder,J., Pratscher,B., Brandt,S., Schneller,D., Mullegger,R., Vogl,C., Trautinger,F., Brem,G. and Burgstaller,J.P. (2015) SNPase-ARMS qPCR: ultrasensitive mutation-based detection of cell-free tumor DNA in melanoma patients. *PLoS One*, **10**, e0142273.
14. Taniguchi,K., Uchida,J., Nishino,K., Kumagai,T., Okuyama,T., Okami,J., Higashiyama,M., Kodama,K., Imamura,F. and Kato,K. (2011) Quantitative detection of EGFR mutations in circulating tumor DNA derived from lung adenocarcinomas. *Clin. Cancer Res.*, **17**, 7808–7815.
15. Pinzani,P., Salvianti,F., Cascella,R., Massi,D., De Giorgi,V., Pazzagli,M. and Orlando,C. (2010) Allele specific Taqman-based real-time PCR assay to quantify circulating BRAF(V600E) mutated DNA in plasma of melanoma patients. *Clin. Chim. Acta*, **411**, 1319–1324.
16. Guha,M., Castellanos-Rizaldos,E. and Makrigiorgos,G.M. (2013) DISSECT method using PNA-LNA clamp improves detection of EGFR T790m mutation. *PLoS One*, **8**, e67782.
17. Abdel-Wahab,O., Klimek,V.M., Gaskell,A.A., Viale,A., Cheng,D., Kim,E., Rampal,R., Bluth,M., Harding,J.J., Callahan,M.K. *et al.* (2014) Efficacy of intermittent combined RAF and MEK inhibition in a patient with concurrent BRAF- and NRAS-mutant malignancies. *Cancer Discov.*, **4**, 538–545.
18. Sanmamed,M.F., Fernandez-Landazuri,S., Rodriguez,C., Zarate,R., Lozano,M.D., Zubiri,L., Perez-Gracia,J.L., Martin-Algarra,S. and Gonzalez,A. (2015) Quantitative cell-free circulating BRAF(V600E) mutation analysis by use of droplet digital PCR in the follow-up of patients with melanoma being treated with BRAF inhibitors. *Clin. Chem.*, **61**, 297–304.
19. Wei,F., Lin,C.C., Joon,A., Feng,Z.D., Troche,G., Lira,M.E., Chia,D., Mao,M., Ho,C.L., Su,W.C. *et al.* (2014) Noninvasive saliva-based EGFR gene mutation detection in patients with lung cancer. *Am. J. Respir. Crit. Care Med.*, **190**, 1117–1126.
20. Nguyen,A.H. and Sim,S.J. (2015) Nanoplasmonic biosensor: detection and amplification of dual bio-signatures of circulating tumor DNA. *Biosens. Bioelectron.*, **67**, 443–449.
21. Das,J., Ivanov,I., Sargent,E.H. and Kelley,S.O. (2016) DNA clutch probes for circulating tumor DNA analysis. *J. Am. Chem. Soc.*, **138**, 11009–11016.
22. Gerasimova,Y.V. and Kolpashchikov,D.M. (2014) Enzyme-assisted target recycling (EATR) for nucleic acid detection. *Chem. Soc. Rev.*, **43**, 6405–6438.
23. Zhao,Y.X., Chen,F., Li,Q., Wang,L.H. and Fan,C.H. (2015) Isothermal amplification of nucleic acids. *Chem. Rev.*, **115**, 12491–12545.
24. Little,J.W. (1967) An exonuclease induced by bacteriophage lambda. II. Nature of the enzymatic reaction. *J. Biol. Chem.*, **242**, 679–686.
25. Kovall,R. and Matthews,B.W. (1997) Toroidal structure of lambda-exonuclease. *Science*, **277**, 1824–1827.
26. Zhang,J.J., McCabe,K.A. and Bell,C.E. (2011) Crystal structures of lambda exonuclease in complex with DNA suggest an electrostatic ratchet mechanism for processivity. *Proc. Natl. Acad. Sci. U.S.A.*, **108**, 11872–11877.

27. Yoo,J. and Lee,G. (2015) Allosteric ring assembly and chemo-mechanical melting by the interaction between 5′-phosphate and lambda exonuclease. *Nucleic Acids Res.*, **43**, 10861–10869.
28. SantaLucia,J. Jr and Hicks,D. (2004) The thermodynamics of DNA structural motifs. *Annu. Rev. Biophys. Biomol. Struct.*, **33**, 415–440.
29. Liu,L., Lei,J., Gao,F. and Ju,H. (2013) A DNA machine for sensitive and homogeneous DNA detection via lambda exonuclease assisted amplification. *Talanta*, **115**, 819–822.
30. Davies,H., Bignell,G.R., Cox,C., Stephens,P., Edkins,S., Clegg,S., Teague,J., Woffendin,H., Garnett,M.J., Bottomley,W. *et al.* (2002) Mutations of the BRAF gene in human cancer. *Nature*, **417**, 949–954.
31. Brose,M.S., Volpe,P., Feldman,M., Kumar,M., Rishi,I., Gerrero,R., Einhorn,E., Herlyn,M., Minna,J., Nicholson,A. *et al.* (2002) BRAF and RAS mutations in human lung cancer and melanoma. *Cancer Res.*, **62**, 6997–7000.
32. Kumar,R., Angelini,S., Czene,K., Sauroja,I., Hahka-Kemppinen,M., Pyrhonen,S. and Hemminki,K. (2003) BRAF mutations in metastatic melanoma: a possible association with clinical outcome. *Clin. Cancer Res.*, **9**, 3362–3368.
33. Fukushima,T., Suzuki,S., Mashiko,M., Ohtake,T., Endo,Y., Takebayashi,Y., Sekikawa,K., Hagiwara,K. and Takenoshita,S. (2003) BRAF mutations in papillary carcinomas of the thyroid. *Oncogene*, **22**, 6455–6457.
34. Ohashi,K., Sequist,L.V., Arcila,M.E., Moran,T., Chmielecki,J., Lin,Y.L., Pan,Y.M., Wang,L., de Stanchina,E., Shien,K. *et al.* (2012) Lung cancers with acquired resistance to EGFR inhibitors occasionally harbor BRAF gene mutations but lack mutations in KRAS, NRAS, or MEK1. *Proc. Natl. Acad. Sci. U.S.A.*, **109**, E2127–E2133.
35. Yuasa,Y., Gol,R.A., Chang,A., Chiu,I.M., Reddy,E.P., Tronick,S.R. and Aaronson,S.A. (1984) Mechanism of activation of an N-Ras oncogene of Sw-1271 human-lung carcinoma-cells. *Proc. Natl. Acad. Sci.-Biol.*, **81**, 3670–3674.
36. Vantveer,L.J., Burgering,B.M.T., Versteeg,R., Boot,A.J.M., Ruiter,D.J., Osanto,S., Schrier,P.I. and Bos,J.L. (1989) N-Ras mutations in human cutaneous melanoma from sun-exposed body sites. *Mol. Cell. Biol.*, **9**, 3114–3116.
37. Irahara,N., Baba,Y., Nosho,K., Shima,K., Yan,L.Y., Dias-Santagata,D., Iafrate,A.J., Fuchs,C.S., Haigis,K.M. and Ogino,S. (2010) NRAS mutations are rare in colorectal cancer. *Diagn. Mol. Pathol.*, **19**, 157–163.
38. Kinsler,V.A., Thomas,A.C., Ishida,M., Bulstrode,N.W., Loughlin,S., Hing,S., Chalker,J., McKenzie,K., Abu-Amero,S., Slater,O. *et al.* (2013) Multiple congenital melanocytic nevi and neurocutaneous melanosis are caused by postzygotic mutations in codon 61 of NRAS. *J. Invest. Dermatol.*, **133**, 2229–2236.
39. Paez,J.G., Jänne,P.A., Lee,J.C., Tracy,S., Greulich,H., Gabriel,S., Herman,P., Kaye,F.J., Lindeman,N., Boggon,T.J. *et al.* (2004) EGFR mutations in lung cancer: correlation with clinical response to gefitinib therapy. *Science*, **304**, 1497–1500.
40. Yarom,N. and Jonker,D.J. (2011) The role of the epidermal growth factor receptor in the mechanism and treatment of colorectal cancer. *Discov Med.*, **11**, 95–105.
41. Costa,R., Shah,A.N., Santa-Maria,C.A., Cruz,M.R., Mahalingam,D., Carneiro,B.A., Chae,Y.K., Cristofanilli,M., Gradishar,W.J. and Giles,F.J. (2017) Targeting Epidermal Growth Factor Receptor in triple negative breast cancer: New discoveries and practical insights for drug development. *Cancer Treat. Rev.*, **53**, 111–119.
42. Zhong,W.Z., Zhou,Q. and Wu,Y.L. (2017) The resistance mechanisms and treatment strategies for EGFR-mutant advanced non-small-cell lung cancer. *Oncotarget*, **8**, 71358–71370.
43. Rotow,J. and Bivona,T.G. (2017) Understanding and targeting resistance mechanisms in NSCLC. *Nat. Rev. Cancer*, **17**, 637–658.
44. Wu,T.B., Xiao,X.J., Gu,F.D. and Zhao,M.P. (2015) Sensitive discrimination of stable mismatched base pairs by an abasic site modified fluorescent probe and lambda exonuclease. *Chem. Commun.*, **51**, 17402–17405.
45. Freier,S.M., Kierzek,R., Caruthers,M.H., Neilson,T. and Turner,D.H. (1986) Free-energy contributions of G.U and other terminal mismatches to helix stability. *Biochemistry-US*, **25**, 3209–3213.
46. SantaLucia,J. (1998) A unified view of polymer, dumbbell, and oligonucleotide DNA nearest-neighbor thermodynamics. *Proc. Natl. Acad. Sci. U.S.A.*, **95**, 1460–1465.
47. Maruyama,T., Takata,T., Ichinose,H., Park,L.C., Kamaiya,N. and Goto,M. (2003) Simple detection of point mutations in DNA oligonucleotides using SYBR Green I. *Biotechnol. Lett.*, **25**, 1637–1641.
48. Asseline,U., Chassignol,M., Aubert,Y. and Roig,V. (2006) Detection of terminal mismatches on DNA duplexes with fluorescent oligonucleotides. *Org. Biomol. Chem.*, **4**, 1949–1957.
49. Chassignol,M., Aubert,Y., Roig,V. and Asseline,U. (2007) Detection of terminal mismatches on DNA duplexes in homogeneous assays or with immobilized probes. *Nucleos. Nucleot Nucl.*, **26**, 1669–1672.
50. Yotapan,N., Nim-anussornkul,D. and Vilaivan,T. (2016) Pyrrolidinyl peptide nucleic acid terminally labeled with fluorophore and end-stacking quencher as a probe for highly specific DNA sequence discrimination. *Tetrahedron*, **72**, 7992–7999.
51. Xiao,X.J., Zhang,C., Su,X., Song,C. and Zhao,M.P. (2012) A universal mismatch-directed signal amplification platform for ultra-selective and sensitive DNA detection under mild isothermal conditions. *Chem. Sci.*, **3**, 2257–2261.
52. Wu,T.B., Xiao,X.J., Zhang,Z. and Zhao,M.P. (2015) Enzyme-mediated single-nucleotide variation detection at room temperature with high discrimination factor. *Chem. Sci.*, **6**, 1206–1211.
53. Xiao,Y., Plakos,K.J.I., Lou,X.H., White,R.J., Qian,J.R., Plaxco,K.W. and Soh,H.T. (2009) Fluorescence detection of single-nucleotide polymorphisms with a single, self-complementary, triple-stem DNA probe. *Angew. Chem.-Int. Ed.*, **48**, 4354–4358.
54. Yang,C.J., Cui,L., Huang,J.H., Yan,L., Lin,X.Y., Wang,C.M., Zhang,W.Y. and Kang,H.Z. (2011) Linear molecular beacons for highly sensitive bioanalysis based on cyclic Exo III enzymatic amplification. *Biosens. Bioelectron.*, **27**, 119–124.
55. Dehe,P.M. and Gaillard,P.H. (2017) Control of structure-specific endonucleases to maintain genome stability. *Nat. Rev. Mol. Cell Biol.*, **18**, 315–330.
56. Lyamichev,V., Brow,M.A. and Dahlberg,J.E. (1993) Structure-specific endonucleolytic cleavage of nucleic acids by eubacterial DNA polymerases. *Science*, **260**, 778–783.
57. Brow,M.A., Oldenburg,M.C., Lyamichev,V., Heisler,L.M., Lyamicheva,N., Hall,J.G., Eagan,N.J., Olive,D.M., Smith,L.M., Fors,L. *et al.* (1996) Differentiation of bacterial 16S rRNA genes and intergenic regions and Mycobacterium tuberculosis katG genes by structure-specific endonuclease cleavage. *J. Clin. Microbiol.*, **34**, 3129–3137.
58. Lyamichev,V., Brow,M.A., Varvel,V.E. and Dahlberg,J.E. (1999) Comparison of the 5′ nuclease activities of taq DNA polymerase and its isolated nuclease domain. *Proc. Natl. Acad. Sci. U.S.A.*, **96**, 6143–6148.
59. Lieber,M.R. (1997) The FEN-1 family of structure-specific nucleases in eukaryotic DNA replication, recombination and repair. *BioEssays*, **19**, 233–240.
60. Harrington,J.J. and Lieber,M.R. (1994) Functional domains within FEN-1 and RAD2 define a family of structure-specific endonucleases: implications for nucleotide excision repair. *Genes Dev.*, **8**, 1344–1355.
61. Lyamichev,V., Mast,A.L., Hall,J.G., Prudent,J.R., Kaiser,M.W., Takova,T., Kwiatkowski,R.W., Sander,T.J., de Arruda,M., Arco,D.A. *et al.* (1999) Polymorphism identification and quantitative detection of genomic DNA by invasive cleavage of oligonucleotide probes. *Nat. Biotechnol.*, **17**, 292–296.
62. Hall,J.G., Eis,P.S., Law,S.M., Reynaldo,L.P., Prudent,J.R., Marshall,D.J., Allawi,H.T., Mast,A.L., Dahlberg,J.E., Kwiatkowski,R.W. *et al.* (2000) Sensitive detection of DNA polymorphisms by the serial invasive signal amplification reaction. *Proc. Natl. Acad. Sci. U.S.A.*, **97**, 8272–8277.
63. Lyamichev,V. and Neri,B. (2003) Invader assay for SNP genotyping. *Methods Mol. Biol.*, **212**, 229–240.
64. Olivier,M. (2005) The Invader assay for SNP genotyping. *Mut. Res.*, **573**, 103–110.